Second order fully semi-Lagrangian discretizations of advection--diffusion--reaction systems

Bonaventura, L.; Carlini, E.; Calzola, E.; Ferretti, R.

Second order
fully semi-Lagrangian discretizations
of advection–diffusion–reaction systems

Luca Bonaventura[1]   Elisabetta Carlini[2]
Elisa Calzola[2] Roberto Ferretti[3]

February 13, 2020

[1] MOX – Modelling and Scientific Computing,
Dipartimento di Matematica, Politecnico di Milano
Via Bonardi 9, 20133 Milano, Italy
luca.bonaventura@polimi.it

[2] Dipartimento di Matematica
Università degli Studi Roma Sapienza
P.le Aldo Moro 5, 00185, Roma, Italy
calzola@mat.uniroma1.it, carlini@mat.uniroma1.it

[3] Dipartimento di Matematica e Fisica
Università degli Studi Roma Tre
L.go S. Leonardo Murialdo 1, 00146, Roma, Italy
ferretti@mat.uniroma3.it

Abstract

We propose a second order, fully semi-Lagrangian method for the numerical solution of systems of advection–diffusion–reaction equations, which employs a semi-Lagrangian approach to approximate in time both the advective and the diffusive terms. Standard interpolation procedures are used for the space discretization on structured and unstructured meshes. The proposed method allows for large time steps, while avoiding the solution of large linear systems, which would be required by an implicit time discretization technique. Numerical experiments demonstrate the effectiveness of the proposed approach and its superior efficiency with respect to more conventional explicit and implicit time discretizations.

1 Introduction

Large systems of advection–diffusion–reaction equations are responsible for most of the computational cost of typical environmental fluid dynamics models, such as are applied in climate modelling, water and air quality models and oceanic biogeochemistry [5], [12], [13]. Also in short and medium range weather forecasting, the number of interacting transported species is significant and drives the choice of optimal time discretization approaches towards methods that allow the use of large time steps [35]. Due to the potentially very large number of equations of this kind that have to be solved simultaneously in order to achieve a complete description of the relevant physical processes, even minor efficiency gains in the discretization of this very classical problem are of paramount practical importance. The standard ways to achieve such optimal efficiency are either the use of implicit schemes, or the application of semi-Lagrangian (SL) techniques, [14], [30] to the advection step, coupled to implicit methods for the diffusion and reaction step. As discussed in [12], [13], SL methods have the advantage that all the computational work that makes them computationally more expensive per time step than standard Eulerian techniques is indeed independent of the number of tracers, which allows to achieve easily a superior efficiency level in the limit of a large number of tracers.

In the recent papers [3], [4], a fully SL approach to both the advection and diffusion step was pursued, which combines the standard SL treatment of advection with SL-like schemes for diffusion, proposed, among others, in [7], [16], [22], [23], [24]. In particular, it was shown in [4] that, even for a single advection–diffusion equation, the fully SL approach can be more efficient than standard implicit techniques.

In the present work, we present a number of improvements to the fully SL approach of [3], [4]. In particular, we show how second order accuracy in time can be achieved. An improved treatment of Dirichlet boundary conditions is also discussed and analysed. The resulting approach yields a very efficient combination, which is validated on a number of classical benchmarks, both on structured and unstructured meshes. Numerical results show that the method yields good quantitative agreement with reference numerical solutions, while being superior in efficiency to standard implicit approaches and to approaches in which the SL method is only used for the advection term.

The outline of the paper is the following. In Section 2, the considered model problems are introduced. Section 3 describes the SL advection–diffusion solver. A stability and convergence analysis of the method is outlined in Section 4. The possible approaches to the

treatment of boundary conditions are discussed in Section 5. A numerical validation of the proposed approach on both structured and unstructured meshes is presented in Section 6, while some conclusions and perspectives for future developments are outlined in Section 7.

2   The model problem

We consider as a model problem the advection–diffusion–reaction equation with Dirichlet boundary conditions

$$
\begin{aligned}
c_t + u \cdot \nabla c - \nu \Delta c = f(c) \qquad & (x,t) \in \Omega \times (0,T], \\
c(x,t) = b(x,t) \qquad & (x,t) \in \partial\Omega \times (0,T], \quad (1) \\
c(x,0) = c_0(x) \qquad & x \in \Omega.
\end{aligned}
$$

The unknown $c : \Omega \times [0,T] \to \mathbb{R}$ can be interpreted as the concentration of a chemical species that is transported through the domain Ω by the advection and diffusion processes, while undergoing locally a nonlinear evolution determined by the source term $f(c)$. T is the final time, $\Omega \subset \mathbb{R}^2$ is an open bounded domain, $u : \Omega \times [0,T] \to \mathbb{R}^2$ is a velocity field and $b : \partial\Omega \times [0,T] \to \mathbb{R}$ denotes the boundary value of the species c. While the proposed numerical method will be presented in this simpler case, the target for more realistic applications are systems of coupled advection–diffusion–reaction equations of the form

$$
\begin{aligned}
(c_k)_t + u \cdot \nabla c_k - \nabla \cdot (D \nabla c_k) = f_k(c_1, \ldots, c_S) \quad & (x,t) \in \Omega \times (0,T], \\
c_k(x,t) = b_k(x,t) \qquad & (x,t) \in \partial\Omega \times (0,T], \qquad (2) \\
c_k(x,0) = c_{0,k}(x) \qquad & x \in \Omega, k = 1, \ldots, S.
\end{aligned}
$$

Here, D denotes a symmetric and positive semi-definite diffusivity tensor, possibly dependent on space and time. As remarked in Section 1, systems of this kind, with a possibly large number of species S, are responsible for the largest share of the computational cost of typical environmental fluid dynamics models, so that even minor increases in the efficiency of the discretization for this very classical problem are of great practical relevance.

3 Fully semi-Lagrangian methods

It can be observed that the evolution equation (1) is of the form

$$c_t = \mathcal{L}c + f(c),$$

where $\mathcal{L}$ denotes a linear differential operator. Consider then the homogeneous equation

$$\tilde{c}_t = \mathcal{L}\tilde{c} \tag{3}$$

associated to (1) with the same initial datum $\tilde{c}(x,0) = c_0(x)$ and boundary conditions as in (1). If the evolution operator determining the solution of (3) is denoted by $\mathcal{E}_t$, so that $\tilde{c}(t) = \mathcal{E}_t[c_0]$, by formal application of the variation of constants formula, the solution of (1) can then be represented as

$$c(x,t) = \mathcal{E}_t[c_0](x) + \int_0^t \mathcal{E}_{t-s}[f \circ c](x) \, \mathrm{d}s. \tag{4}$$

If discrete time levels $t_n, n = 0, \ldots, N$ are introduced, so that $t_n = n\Delta t$ and $\Delta t = T/N$, a numerical method for the solution of equation (1) on the interval $[t_n, t_{n+1}]$ can then be derived from the representation formula

$$c(x,t_{n+1}) = \mathcal{E}_{\Delta t}[c(.,t_n)](x) + \int_{t_n}^{t_{n+1}} \mathcal{E}_{t_{n+1}-s}[f \circ c](x) \, \mathrm{d}s. \tag{5}$$

Discretizing the time integral by the trapezoidal rule, one obtains

$$
\begin{aligned}
c(x,t_{n+1}) &\approx \mathcal{E}_{\Delta t}[c(.,t_n)](x) \\
&\quad + \frac{\Delta t}{2}\left[\mathcal{E}_{\Delta t}[f \circ c](x) + f(c(x,t_{n+1}))\right].
\end{aligned} \tag{6}
$$

If the diffusion term is dropped in equation (1) and the evolution operator is approximated by a numerical approximation of the flow streamline and an interpolation at the departure point of the streamline, a numerical method based on formula (6) can be interpreted as a semi-Lagrangian extension of the trapezoidal rule with global truncation error of order 2. Semi-Lagrangian methods based on this formula have been used successfully in a large number of applications, see, among many others, [1],[10],[11],[31],[32],[34]. Often, a first order, off-centered version of the above formula is employed, defined for $\theta \in [1/2, 1]$ by

$$
\begin{aligned}
c(x,t_{n+1}) &\approx \mathcal{E}_{\Delta t}[c(.,t_n)](x) \\
&\quad + (1-\theta)\Delta t \mathcal{E}_{\Delta t}[f \circ c](x) + \theta \Delta t f(c(x,t_{n+1})).
\end{aligned} \tag{7}
$$

The goal of this work is to extend this approach to the case of a semi-Lagrangian treatment of both advection and diffusion terms. In order to do this, we introduce a spatial discretization mesh $\mathcal{G}_{\Delta x} = \{x_i, \ x_i \in \Omega\}$, where Δx denotes a measure of the mesh resolution. Notice that the only necessary restriction on the nature of the mesh is that it should be possible to define a polynomial interpolation operator $I_p[c](\cdot)$ of degree p, constructed on the values of a grid function c defined on $\mathcal{G}_{\Delta x}$. Assuming in the following that such operator is defined on structured and unstructured meshes (for the definition of such interpolation operator see for instance [27]), examples of applications using both meshes will be considered.

We then denote the discrete approximations of the solution of (1) at the space-time mesh nodes by c_i^n and by

$$z_i^{n+1} = X_{\Delta t}(x_i, t_{n+1}; t_n) \tag{8}$$

some numerical approximations of the streamlines starting at x_i and defined by the velocity field u over the interval $[t_n, t_{n+1}]$. In particular, in [3],[4] explicit Euler or Heun methods were employed to compute these approximations, coupled to a substepping approach along the lines of [9],[29]. More specifically, for the Euler method, given a positive integer m, a time substep was defined as $\Delta\tau = \Delta t/m$ and, for $q = 0, \ldots, m-1$,

$$\begin{aligned} y^{(q+1)} &= y^{(q)} - \Delta\tau u(y^{(q)}, t_n), \\ y^{(0)} &= x_i \end{aligned} \tag{9}$$

was computed, so that $z_i^{n+1} = y^m$. Following the approach outlined in [3] and applied in [4], a first order in time approximation of the solution of (1) can then be defined as

$$c_i^{n+1} = \frac{1}{4}\sum_{k=1}^{4} I_p[c^n]\left(z_i^{n+1} + \delta_k\right) \tag{10}$$

$$+ (1-\theta)\Delta t \frac{1}{4}\sum_{k=1}^{4} f(I_p[c^n])\left(z_i^{n+1} + \delta_k\right) + \theta\Delta t f(c_i^{n+1}),$$

where $c^n = (c^n)_i$. In (10), δ_k is defined, for $k = 1, \ldots, 4$, as

$$\delta_k = \pm\delta e_j$$

(e_j ($j = 1, 2$) denoting the canonical basis in $\mathbb{R}^2$), for all combination of both the sign and the index $j = 1, 2$; moreover, $\delta = \sqrt{4\nu\Delta t}$.

Notice that, for simplicity, we neglect in (10) the treatment of boundary conditions. Possible approaches to handle nontrivial boundary conditions will be discussed in Section 5.

The method (10) will be denoted in what follows by SL1. This method inherits the same stability and convergence properties of the parent methods, as it will be discussed in Section 4. Notice that this approach can be extended to spatially varying diffusion coefficients and that, while only first order in time, its effective accuracy can be substantially superior to that of more standard techniques, if higher degree interpolation operators are used, as shown in [3].

In order to derive a method of second order in time, we follow the main steps of [16],[25]. The streamlines are interpreted as generalized characteristics, defined as the solutions of the stochastic differential equation:

$$dX = -u(X(s), s)ds + \sigma dW(s), \quad X(t_{n+1}) = x_i$$

for $s \in [0, \Delta t]$, $\sigma = \sqrt{2\nu}$, where $W(s)$ denotes a standard 2-dimensional Wiener process. Applying the implicit weak method of order 2 defined in [19] for the approximation of the streamlines, we denote by

$$z_{k,i}^{n+1} = X_{\Delta t}^k(x_i, t_{n+1}; t_n) \quad (k = 1, \ldots, 9) \tag{11}$$

the solutions of the nonlinear equations

$$z_{k,i}^{n+1} = x_i - \frac{\Delta t}{2}\left(u(x_i, t_{n+1}) + u(z_{k,i}^{n+1}, t_n)\right) + \sqrt{3\Delta t}\sigma e_k. \tag{12}$$

Here, e_k denote the vectors:

$$e_1 = \begin{pmatrix} 0 \\ 0 \end{pmatrix}, \quad e_2 = \begin{pmatrix} 0 \\ 1 \end{pmatrix}, \quad e_3 = \begin{pmatrix} 0 \\ -1 \end{pmatrix},$$

$$e_4 = \begin{pmatrix} 1 \\ 0 \end{pmatrix}, \quad e_5 = \begin{pmatrix} -1 \\ 0 \end{pmatrix}, \quad e_6 = \begin{pmatrix} 1 \\ 1 \end{pmatrix},$$

$$e_7 = \begin{pmatrix} 1 \\ -1 \end{pmatrix}, \quad e_8 = \begin{pmatrix} -1 \\ 1 \end{pmatrix}, \quad e_9 = \begin{pmatrix} -1 \\ -1 \end{pmatrix}.$$

These vectors represent a realization of a vector random variable whose distribution is given by the probabilities

$$\alpha_1 = 4/9, \quad \alpha_2 = \alpha_3 = \alpha_4 = \alpha_5 = 1/9, \quad \alpha_6 = \alpha_7 = \alpha_8 = \alpha_9 = 1/36.$$

It is to be remarked that method (12) can be rewritten in terms of the displacements $\delta_{k,i}^{n+1} = z_{k,i}^{n+1} - x_i$ as

$$\delta_{k,i}^{n+1} = -\frac{\Delta t}{2}\left(u(x_i, t_{n+1}) + u(x_i + \delta_{k,i}, t_n)\right) + \sqrt{3\Delta t}\sigma e_k, \tag{13}$$

thus yielding an implicit method that is a natural extension to stochastic differential equations of that introduced in [28] and commonly used

7

in meteorological applications for the computation of streamlines in SL methods. A second order in time SL (SL2) scheme can then be defined by a Crank-Nicolson approach as

$$c_i^{n+1} = \sum_{k=1}^{9} \alpha_k \left(I_p[c^n](z_{k,i}^{n+1}) + \frac{\Delta t}{2} f(I_p[c^n](z_{k,i}^{n+1})) \right)$$
$$+ \frac{\Delta t}{2} f(c_i^{n+1}). \tag{14}$$

Notice that, with respect to the simpler first order in time variant (10), nine interpolations at the foot of the streamlines must be computed, which clearly makes this approach substantially more expensive than the simpler, first order in time variant. In applications to systems of the form (2), the computational cost of scheme (14) can be marginally reduced by setting

$$\tilde{c}_i^n = \sum_{k=1}^{9} \alpha_k I_p[c^n](z_{k,i}^{n+1})$$

and defining

$$c_i^{n+1} = \tilde{c}_i^n + \frac{\Delta t}{2} f(\tilde{c}_i^n) + \frac{\Delta t}{2} f(c_i^{n+1}), \tag{15}$$

so as to reduce the number of the evaluations of a possibly costly nonlinear term. Furthermore, when the coupling of the diffusion and advection term is weak, it should be possible to decouple again the approximation of a single deterministic streamline from that of the diffusive displacements, which could be added at the end of each approximate streamline without increasing too much the error. The deterministic streamline can then be computed by a substepping procedure, applied either to explicit methods as in (9) or to implicit methods as in (12).

For example, a decoupled substepping variant of (12) might be obtained by computing, for $q = 0, \ldots, m-1$,

$$y^{(q+1)} = y^{(q)}$$
$$- \frac{\Delta \tau}{2} \left[u(y^{(q)}, t_{n+1} - q\Delta \tau) + u(y^{(q+1)}, t_{n+1} - (q+1)\Delta \tau) \right],$$
$$y^0 = x_i, \tag{16}$$

and setting $z_k = y^m + \sqrt{3\Delta t}\sigma e_k$. We will denote this decoupled variant with substepping by SL2s.

Notice that, in realistic problems, a bottleneck of the scheme (14) is the fact that the Crank–Nicolson method, while A-stable, is not L-stable, see e.g. [20]. Therefore, no damping is introduced by the

method for very large values of the time step and spurious oscillations may arise, see also the discussion in [6]. In order to reduce the computational cost and to address the L-stability issue, different variants of the (14) scheme could also be introduced and compared, along the lines proposed in [33] for the pure advection case. However, this development goes beyond the scope of this paper and will not be pursued here.

Finally, even though achieving full second order consistency is quite complicated in the variable diffusion coefficient case, the previously introduced schemes can be nonetheless extended at least in the simpler configurations as suggested in [3] for the first order case, even though full second order accuracy is not guaranteed any more.

4   Convergence analysis

We present in this section a convergence analysis for the scheme (14). For simplicity, we assume a one-dimensional problem defined on $\mathbb{R} \times [0, T]$, with a time-independent drift term u:

$$
\begin{cases}
c_t + u(x)c_x - \nu c_{xx} = f(c) & (x, t) \in \mathbb{R} \times (0, T], \\
c(x, 0) = c_0(x) & x \in \mathbb{R}.
\end{cases}
\tag{17}
$$

The multidimensional case, as well as the time dependence of u, require only small technical adaptations. On the other hand, the convergence analysis on bounded domains is still an open problem for high-order SL schemes, therefore we will not address this problem here.

First, for $i \in \mathbb{Z}$ and $n = 0, \dots, N-1$, we rewrite the scheme (14) with the shorthand notation

$$
c_i^{n+1} = S_{\Delta t, \Delta x}\left(c^{n+1}, c^n, x_i\right),
\tag{18}
$$

where $x_i = i\Delta x$, and

$$
\begin{aligned}
S_{\Delta t, \Delta x}\left(c^{n+1}, c^n, x_i\right) \;=\; & \sum_k \alpha_k \left[I_p[c^n](z_k(x_i)) + \frac{\Delta t}{2} f(I_p[c^n](z_k(x_i)))\right] \\
& + \frac{\Delta t}{2} f\left(c_i^{n+1}\right).
\end{aligned}
$$

In one space dimension, the three discrete characteristics are defined by the equations

$$
\begin{aligned}
z_+(x) &= x - \frac{\Delta t}{2}[u(x) + u(z_+(x))] + \sqrt{6\Delta t}\nu, \\
z_-(x) &= x - \frac{\Delta t}{2}[u(x) + u(z_-(x))] - \sqrt{6\Delta t}\nu, \\
z_0(x) &= x - \frac{\Delta t}{2}[u(x) + u(z_0(x))],
\end{aligned}
$$

with corresponding weights $\alpha_+ = \alpha_- = 1/6$ and $\alpha_0 = 2/3$. In what follows, we will use the symbol K to denote various positive constants, which do not depend on $\Delta t, x, t$. We will also assume that:

(H0) there exists a unique classical solution of (17);

(H1) $f(x) \in C^4(\mathbb{R})$ with $|f^{(p)}(x)| \leq K$ for $p \leq 4$;

(H2) $u(x) \in C^2(\mathbb{R})$ with $|u^{(p)}(x)| \leq K$ for $p \leq 2$;

(H3) for any $v(x) \in C^{p+1}(\mathbb{R})$ with bounded derivatives, $I_p[v]$ is a piecewise polynomial interpolation operator such that for any $x \in \mathbb{R}$
$$
|I_p[v](x) - v(x)| \leq K\Delta x^p.
$$

4.1 Consistency

First, we derive a consistency result via a Taylor expansion. The same kind of result can be obtained by probabilistic arguments, see [23].

Proposition 1. *Assume* **(H1)***–***(H3)***, and let $c(x,t)$ be a smooth solution of (17). Then, for each $(i,n) \in \mathbb{Z} \times \{0, \ldots, N-1\}$ the consistency error of the scheme (14), defined as*

$$
\mathcal{T}_{\Delta t, \Delta x}(x_i, t_n) = \frac{1}{\Delta t}\left(c(x_i, t_{n+1}) - S_{\Delta t, \Delta x}\left(c(t_n), c(t_{n+1}), x_i\right)\right)
$$

where $c(t_n) = (c(x_i, t_n))_i$, is such that

$$
\mathcal{T}_{\Delta t, \Delta x}(x, t) = \mathcal{O}\left(\Delta t^2 + \frac{\Delta x^p}{\Delta t}\right).
$$

Proof. In what follows, we will omit the argument of functions computed at (x, t). Consider a smooth solution c of (17). Since assumption **(H1)** holds, by differentiating in time and space (17) we get that c is also solution of

$$
c_{tt} + u(x)c_{xt} - \nu c_{xxt} = f'(c)c_t, \tag{19}
$$

$$
c_{tx} + u'(x)c_x + u(x)c_{xx} - \nu c_{xxx} = f'(c)c_x, \tag{20}
$$

10

and hence, by differentiating again in space (20), of

$$c_{txx} + u''(x)c_x + u'(x)c_{xx} + u'(x)c_{xx} + u(x)c_{xxx} - \nu c_{xxxx}$$
$$= f''(c)(c_x)^2 + f'(c)c_{xx}. \tag{21}$$

Using (20) and (21) in (19), we get :

$$
\begin{aligned}
c_{tt} &= uu'c_c + u^2 c_{xx} - u\nu c_{xxx} - \nu u''c_x - 2\nu u'c_{xx} - u\nu c_{xxx} + \nu^2 c_{xxxx} \\
&= (uu' - \nu u')\,c_x + (u^2 - 2\nu u')\,c_{xx} - 2u\nu c_{xxx} + \nu^2 c_{xxxx} \\
&\quad + f'(c)(c_t - uc_x + \nu c_{xx}) + \nu f''(c)(c_x)^2. \tag{22}
\end{aligned}
$$

Define now $U_\pm(x) = u(x) + u(z_\pm(x))$. By a Taylor expansion of $c(z_\pm(x), t)$ in space around (x, t), we obtain

$$
\begin{aligned}
c(z_\pm(x), t) &= c + \left(\pm\sqrt{6\Delta t\nu} - \frac{\Delta t}{2}U_\pm\right)c_x + \frac{1}{2}\left(\pm\sqrt{6\Delta t\nu} - \frac{\Delta t}{2}U_\pm\right)^2 c_{xx} \\
&\quad + \frac{1}{6}\left(\pm\sqrt{6\Delta t\nu} - \frac{\Delta t}{2}U_\pm\right)^3 c_{xxx} \\
&\quad + \frac{1}{24}\left(\pm\sqrt{6\Delta t\nu} - \frac{\Delta t}{2}U_\pm\right)^4 c_{xxxx} \\
&\quad + \frac{1}{120}\left(\pm\sqrt{6\Delta t\nu} - \frac{\Delta t}{2}U_\pm\right)^5 c_{xxxxx} + \mathcal{O}(\Delta t^3) \tag{23}
\end{aligned}
$$

and, defining $U_0(x) = u(x) + u(z_0(x))$,

$$c(z_0(x), t) = c - \frac{\Delta t}{2}U_0 c_x + \frac{1}{2}\left(-\frac{\Delta t}{2}U_0\right)^2 c_{xx} + \mathcal{O}(\Delta t^3). \tag{24}$$

Using (22),(23),(24) and the Taylor expansion

$$c(x, t + \Delta t) = c + \Delta t c_t + \frac{\Delta t^2}{2}c_{tt} + \mathcal{O}(\Delta t^3),$$

we obtain

$$
\begin{aligned}
c(x, t + \Delta t) \quad &- \quad \sum_k \alpha_k c(z_k(x), t) = \Delta t(c_t + u(x)c_x - \nu c_{xx}) \\
&+ \quad \frac{\Delta t^2}{2}(f'(c)(c_t - uc_x + \nu c_{xx}) + \nu f''(c)(c_x)^2) \\
&+ \quad \mathcal{O}(\Delta t^3). \tag{25}
\end{aligned}
$$

Consider now the nonlinear reaction term. By assumption **(H3)**, we have that

$$
\begin{aligned}
f(c(z, t)) &= f(c) + f'(c)(c(z, t) - c) + \frac{1}{2}f''(c)(c(z, t) - c)^2 \\
&\quad + \frac{1}{6}f'''(c)(c(z, t) - c))^3 + \mathcal{O}((c(z, t) - c)^4) \tag{26}
\end{aligned}
$$

11

Using (25) in (26), and taking into account that $c(z_\pm, t) = c \pm \sqrt{6\Delta t \nu} c_x +$
$\mathcal{O}(\Delta t)$ and $c(z_0(x), t) = c + \mathcal{O}(\Delta t)$, we obtain

$$
\begin{aligned}
\sum_k (\alpha_k f(c(z_k(x), t))) &= f(c) + f'(c) \left(c(x, t + \Delta t) - \Delta t(c_t + u c_x - \nu c_{xx}) - c \right) \\
&+ f''(c)(\Delta t \nu c_x^2) + \mathcal{O}(\Delta t^2).
\end{aligned}
\tag{27}
$$

By (27) and (25), we get the consistency error for the semi-discretization,

$$
\begin{aligned}
c(x, t + \Delta t) &- \sum_k \alpha_k \left(c(z_k(x), t) + \frac{\Delta t}{2} f(c(z_k(x), t)) \right) \\
&- \frac{\Delta t}{2} f(c(x, t + \Delta t)) \\
&= \Delta t(c_t + u(x) c_x - \nu c_{xx} - f(c)) + \mathcal{O}\left(\Delta t^3\right). \tag{28}
\end{aligned}
$$

Introducing the interpolation error and using assumptions **(H2)** and **(H1)**, we finally prove the consistency error for the fully discrete scheme. $\qquad \square$

4.2 Stability

To prove stability, it is convenient to recast (18) in the matrix form

$$
c^{n+1} - \frac{\Delta t}{2} f\left(c^{n+1}\right) = \sum_k \alpha_k \left[B_k c^n + \frac{\Delta t}{2} f\left(B_k c^n\right) \right],
$$

where, for a vector c, $f(c)$ denotes the vector obtained by applying f elementwise and the matrices B_k (which represent the operation of interpolating c^n at the points $z_k(x_i)$) have elements $b_{k,ij}$ defined by

$$
b_{k,ij} = \psi_j(z_k(x_i)), \tag{29}
$$

for a suitable basis of cardinal functions $\{\psi_j\}$. The following proposition implies stability for the linear part of the scheme with respect to the 2-norm. For a formal definition of the basis functions ψ_j we refer the reader to [17], [18].

Proposition 2. *Assume* **(H2)**, *and let the matrix B have elements defined by (29), with (ψ_j) basis functions for odd degree symmetric Lagrange or splines interpolation. Then, for each k, there exists a constant $K_B > 0$ independent on $\Delta x, \Delta t$ such that*

$$
\|B_k\| \leq 1 + K_B \Delta t. \tag{30}
$$

Proof. If we adopt a piecewise linear interpolation, the scheme is monotone and satisfies (30) both in the ∞-norm (with $K_B = 0$) and in the 2-norm, see for example [17]. We will therefore focus on the case of high-order interpolations, for which the norm in (30) should be understood as 2-norm. Following [17], [18], we sketch the arguments to prove (30) for the cases of symmetric Lagrange and splines interpolation, which can be interpreted as Lagrange–Galerkin schemes with area-weighting. First, we make explicit the dependence of the points z_k on x and Δt. We recall that $z_k(x) = x + \delta_k(x)$, with δ_k solving the equation:

$$\delta_k(x) = -\frac{\Delta t}{2} \left(u(x) + u(x + \delta_k(x)) \right) + \sqrt{3\Delta t}\sigma e_k.$$

Expanding the term $u(x + \delta_k(x))$, we obtain therefore

$$\delta_k(x) = -\frac{\Delta t}{2} \left(u(x) + u(x) + \delta_k u'(x) \right) + \mathcal{O}\left(\delta_k^2\right)\right) + \sqrt{3\Delta t}\sigma e_k,$$

and hence,

$$\delta_k(x) \left(1 + \frac{\Delta t}{2} u'(x) \right) = -\Delta t\, u(x) + \sqrt{3\Delta t}\sigma e_k + \mathcal{O}\left(\Delta t \delta_k^2\right).$$

Dividing now by $1 + \Delta t\, u'/2$, and using the fact that $\delta_k = \mathcal{O}(\sqrt{\Delta t})$, we get, for $\Delta t \to 0$,

$$z_k(x) = x - \Delta t\, u(x) + \sqrt{3\Delta t}\sigma e_k + \mathcal{O}\left(\Delta t^2\right). \tag{31}$$

Due to the term $\sqrt{3\Delta t}\sigma e_k$, the form of (31) does not coincide with that used in [17] for the points $z_k(x)$. However, when considering differences $z_k(x_1) - z_k(x_2)$, this additional term is cancelled, so that

$$z_k(x_1) - z_k(x_2) = (x_1 - x_2) - \Delta t(u(x_1) - u(x_2)) + \mathcal{O}\left(\Delta t^2\right).$$

As a consequence, the form (31) still satisfies the relevant properties used in the proof of (30). In particular, it satisfies the condition [17, Lemma 3]

$$|z_k(x_1) - z_k(x_2)| \geq \frac{1}{2}|x_1 - x_2|,$$

for Δt small enough, as well as the condition [17, Theorem 4]

$$|z_k(x_1) - (x_1 - x_2 + z_k(x_2))| \leq K_X|x_1 - x_2|\Delta t,$$

for a suitable positive constant K_X. Then, a careful replica of the arguments used in [17] provides the estimate (30). $\qquad\square$

4.3 Convergence

We now present a convergence result in the discrete 2-norm.

Theorem 3. *Assume* **(H0)**–**(H3)**. *Let* $c(x, t)$ *be the classical solution of* (17), *and* c^n *be the solution of* (18). *Then, for any* n *such that* $t_n \in [0, T]$ *and for* $(\Delta t, \Delta x) \to 0$,

$$\|c(t_n) - c^n\|_2 \leq K_T \left(\Delta t^2 + \frac{\Delta x^p}{\Delta t} \right),$$

where K_T *is positive constant depending on the final time* T.

Proof. While a mere convergence proof could be carried out with weaker regularity assumptions, we will focus here on the error estimate above, which require the regularity assumed in **(H0)**–**(H3)**. Define the vectors γ^n and ν^n, so that $\gamma_i^n = c(x_i, t_n)$, and $\epsilon^n = \gamma^n - c^n$. Then, by Proposition 1, we get

$$\gamma^{n+1} - \frac{\Delta t}{2} f\left(\gamma^{n+1}\right) = \sum_k \alpha_k \left[B_k^n \gamma^n + \frac{\Delta t}{2} f\left(B_k^n \gamma^n\right) \right]$$
$$+ \mathcal{O}(\Delta t^3 + \Delta x^p). \tag{32}$$

Subtracting (18) from (32), using the Lipschitz continuity of f and the triangle inequality in the form of a difference, we obtain from the left-hand side:

$$\left\| \gamma^{n+1} - \frac{\Delta t}{2} f\left(\gamma^{n+1}\right) - c^{n+1} + \frac{\Delta t}{2} f\left(c^{n+1}\right) \right\|_2 \geq \left(1 - \frac{L_f \Delta t}{2}\right) \|\epsilon^{n+1}\|_2.$$

Taking into account that $\sum_k \alpha_k = 1$, along with the bound (30), we also have from the right-hand side:

$$\left\| \gamma^{n+1} - \frac{\Delta t}{2} f\left(\gamma^{n+1}\right) - c^{n+1} + \frac{\Delta t}{2} f\left(c^{n+1}\right) \right\|_2$$
$$\leq \left(1 + \frac{L_f \Delta t}{2}\right) (1 + K_B \Delta t) \|\epsilon^n\|_2 + \mathcal{O}(\Delta t^3 + \Delta x^p).$$

Therefore, it turns out that

$$\left(1 - \frac{L_f \Delta t}{2}\right) \|\epsilon^{n+1}\|_2 \leq \left(1 + \frac{L_f \Delta t}{2}\right) (1 + K_B \Delta t) \|\epsilon^n\|_2$$
$$+ \mathcal{O}(\Delta t^3 + \Delta x^p). \tag{33}$$

Now, for Δt small enough to have $1 - L_f \Delta t / 2 > \underline{C} > 0$, we have that there exists a constant $K_T > 0$ such that

$$\frac{1 + \dfrac{L_f \Delta t}{2}}{1 - \dfrac{L_f \Delta t}{2}} (1 + K_B \Delta t) \leq 1 + K_T \Delta t,$$

and hence, using this bound in (33),

$$\left\|\epsilon^{n+1}\right\|_2 \le (1 + K_T \Delta t) \left\|\epsilon^n\right\|_2 + \mathcal{O}(\Delta t^3 + \Delta x^p), \qquad (34)$$

which, by standard arguments, implies that, for any n such that $t_n \in [0, T]$,

$$\|\epsilon^n\|_2 \le K_T \left(\Delta t^2 + \frac{\Delta x^p}{\Delta t} \right).$$

$\square$

5   Boundary conditions

The treatment of Dirichlet boundary conditions for this class of semi-Lagrangian methods has been considered in [24], where two methods are proposed. One approach has first order of consistency, but it does not seem possible to generalize it to multiple dimensions. The second approach has order of consistency $1/2$. More recently, in [4], an easier treatment has been proposed for the scheme SL1 with time-independent Dirichlet boundary condition, again with order of consistency $1/2$. This approach has been extended in [2] to unstructured meshes.

We propose here a new approach to obtain second order consistency for the scheme SL2 with Dirichlet boundary conditions. This technique is based on extrapolation, much in the spirit of the so-called *ghost-point* techniques, see e.g. [21].

In addition to the standard mesh $\mathcal{G}_{\Delta x} = \{x_i, \ x_i \in \overline{\Omega}\}$, where the numerical solution is computed, we consider a second mesh $\mathcal{G}_h = \{v_i, \ v_i \in \overline{\Omega}\}$ formed by a single layer of elements having their external side along the boundary of Ω. This second mesh is constructed with a size parameter $h \sim \sqrt{\Delta t}$, and the degrees of freedom are chosen in order to allow a second-order interpolation. In Fig.1 we show, as an example, a square domain $\Omega = (-1, 1) \times (-1, 1)$, for which the standard mesh $\mathcal{G}_{\Delta x}$ is formed by the blue triangular elements and the mesh $\mathcal{G}_h$ is formed by the black rectangular elements. Note that the latter overlap at the corners. The asterisks in red are the nodes of $\mathcal{G}_h$, according to the standard $\mathbb{Q}_2$ element. The values of the numerical solution on the nodes v_i are obtained by interpolation at internal nodes, and by the Dirichlet boundary condition if the nodes lie on the boundary $\partial\Omega$.

Let us call $\mathcal{T}_{\Delta x}$ a given triangulation, with $\mathcal{G}_{\Delta x}$ the set of the vertexes of the elements $K \in \mathcal{T}_{\Delta x}$. Let us define the polygonal domain $\Omega_{\Delta x} := \cup_{K \in \tau_{\Delta x}} K \subset \Omega$. If, for some i and k, $z_{k,i}^{n+1} \notin \overline{\Omega}_{\Delta x}$, then its projection $P(z_{k,i}^{n+1})$ onto $\overline{\Omega}_{\Delta x}$ is computed, defined as the point in $\overline{\Omega}_{\Delta x}$
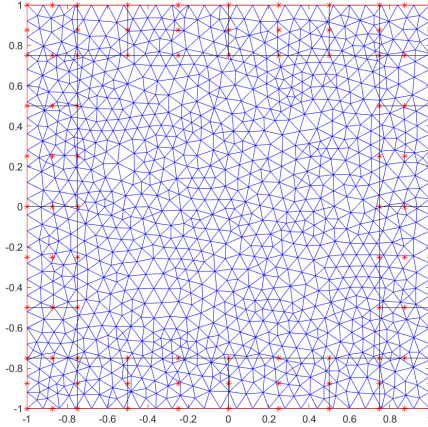
Figure 1: Unstructured computational mesh (blue triangular elements) together with boundary mesh $\mathcal{G}_h$ (black rectangular elements and red asterisks nodes)

at minimum distance from $z_{k,i}^{n+1}$. The value of the numerical solution $c^n(z_{k,i}^{n+1})$ is then approximated by a quadratic extrapolation operator Ψ_2. This operator is constructed via the $\mathbb{Q}_2$ associated to the element of $\mathcal{G}_h$ to which the projection $P(z_{k,i}^{n+1})$ belongs:

$$c^n(z_{k,i}^{n+1}) \simeq \Psi_2[\hat{c}^n](z_{k,i}^{n+1})),$$

where $\hat{c}^n$ corresponds to

$$\hat{c}^n(v_i) = \begin{cases} I_2[c^n](v_i) & \text{if } v_i \in \Omega, \\ b(v^i, t_n) & \text{if } v_i \in \partial\Omega. \end{cases}$$

The method can be extended to more general domains, by considering triangular elements for $\mathcal{G}_h$. This technique will not be rigorously analysed here, but we will provide a numerical validation in Section 6.5.

6 Numerical results

A number of numerical experiments have been carried out, in order to assess the accuracy of the proposed methods on both structured and unstructured meshes. In the unstructured case, we have constructed a triangular mesh by the Matlab2019 function `generateMesh`, with a maximum mesh edge of Δx, and used a $\mathbb{P}_2$ space reconstruction. In

16

the structured Cartesian case, the bicubic polynomial interpolation implemented in the Matlab2019 command `interp2`, has been used. Since the goal is to evaluate the accuracy of time discretization, both choices avoid to hide the time discretization error with the error introduced by a lower order space reconstruction.

6.1 Pure diffusion

In a first, basic test, we consider equation (1) in the pure diffusion case, i.e., with zero advection and reaction terms, on the square domain $\Omega = (-2, 2) \times (-2, 2)$, with $T = 1$ and $\nu = 0.05$. Based on the test case proposed in [26], we assume a Gaussian initial datum centered in $(0, 0)$, with $\sigma = 0.1$, so that the exact solution in an infinite plane would be

$$c(x, y, t) = \frac{1}{1 + 2\nu t/\sigma^2} \exp\left\{-\frac{x^2 + y^2}{2(\sigma^2 + 2\nu t)}\right\}.$$

For this test case, we only consider structured meshes with constant steps $\Delta x = \Delta y = 4/N$ in both directions. Following [3], we consider different time step values Δt, which correspond to different values of the parabolic stability parameter $\mu = \Delta t \nu/\Delta x^2$. We compare method SL1 (10) and method SL2 (14), and collect the results in Table 1. It can be observed that the expected convergence rates are recovered. Furthermore, it is apparent that scheme SL2 yields a substantial accuracy improvement, without an excessive increase in computational cost. Indeed, the SL2 runs require between 30% and 60% more CPU time, depending on the resolution, while leading to corresponding error reductions between 140% and 730%. As a comparison, a standard second order discretization in space coupled to an explicit second order method in time yields at the finest resolution an error 5 times larger than that of method SL2 at approximately the same computational cost.

6.2 Solid body rotation

Next, we consider the advection–diffusion equation (1) with coefficients $u = (-\omega y, \omega x)$, $\omega = 2\pi$, $\nu = 0.05$ and $f = 0$ on the square domain $\Omega = (-2, 2) \times (-2, 2)$ and $T = 1$. Following [26], we assume a Gaussian initial datum centered at $(x_0, y_0) = (1, 0)$ with $\sigma = 0.05$, so that the exact solution in an infinite plane would be

$$c(x, y, t) = \frac{1}{1 + 2\nu t/\sigma^2} \exp\left\{-\frac{(x - x(t))^2 + (y - y(t))^2}{2(\sigma^2 + 2\nu t)}\right\}, \quad (35)$$

Resolution		Relative error		Convergence rates	
Δx	μ	l_2	l_∞	p_2	p_∞
0.08	0.84	$3.34 \cdot 10^{-2}$	$5.10 \cdot 10^{-2}$	-	-
0.04	1.6	$1.33 \cdot 10^{-2}$	$2.05 \cdot 10^{-2}$	1.33	1.00
0.02	3.2	$6.57 \cdot 10^{-3}$	$1.03 \cdot 10^{-2}$	1.02	0.99

Resolution		Relative error		Convergence rates	
Δx	μ	l_2	l_∞	p_2	p_∞
0.08	0.84	$2.66 \cdot 10^{-3}$	$4.76 \cdot 10^{-3}$	-	-
0.04	1.6	$4.89 \cdot 10^{-4}$	$8.24 \cdot 10^{-4}$	2.44	2.53
0.02	3.2	$8.89 \cdot 10^{-5}$	$1.48 \cdot 10^{-4}$	2.46	2.48

Table 1: Errors for the pure diffusion test, first order method SL1 (upper) and second order method SL2 (lower) on a structured mesh.

where $x(t) = x_0 \cos \omega t - y_0 \sin \omega t$, $y(t) = x_0 \sin \omega t - y_0 \cos \omega t$. We first consider structured meshes with constant steps $\Delta x = \Delta y = 4/N$ in both coordinate directions. We consider again values of Δt corresponding to different values of the parabolic stability parameter μ, as well as of the Courant number $\lambda = \Delta t \max |u| / \Delta x$.

In the structured case, we compare method SL1 (10) with Euler substepping as in (9), the decoupled variant SL2s of method (14) with Heun substepping, and method SL2 (14) with the fully coupling (13). The results are reported in Table 2, in which convergence rates are computed with respect to the values in the first row. Furthermore, the convergence rate estimation for the values in the last row takes into account that the time step has been reduced by a factor 4.

It can be observed that the expected convergence rates with respect to the time discretization error are recovered, in the constant Δx, constant C or constant μ convergence studies. It can also be observed that the decoupled variant SL2s, in spite of the loss of second order convergence, does indeed improve the results with respect to the SL1 method and is competitive with the full second order method SL2. As a comparison, a standard centered finite difference, second order discretization in space coupled to an explicit second order method in time yields at the finest resolution an error analogous to that of method SL2 but requires approximately three times its CPU time.

In the unstructured case, the quadratic polynomial interpolation naturally associated to $\mathbb{P}_2$ finite elements was employed and only the SL2s and SL2 methods were considered. The triangular mesh used was chosen with maximum triangle size Δx approximately equal to the corresponding structured meshes. The results are reported in Table 3.

18

Resolution			Relative error		Convergence rates	
Δx	λ	μ	l_2	l_∞	p_2	p_∞
0.04	16	1.62	0.15	0.16	-	-
0.04	8	0.82	$7.71 \cdot 10^{-2}$	$8.13 \cdot 10^{-2}$	0.96	0.98
0.02	16	3.2	$7.71 \cdot 10^{-2}$	$8.13 \cdot 10^{-2}$	0.96	0.98
0.02	8	1.6	$3.92 \cdot 10^{-2}$	$4.13 \cdot 10^{-2}$	0.97	0.97

Resolution			Relative error		Convergence rates	
Δx	λ	μ	l_2	l_∞	p_2	p_∞
0.04	16	1.62	$7.65 \cdot 10^{-2}$	$7.95 \cdot 10^{-2}$	-	-
0.04	8	0.82	$3.89 \cdot 10^{-2}$	$4.02 \cdot 10^{-2}$	0.98	0.98
0.02	16	3.2	$3.89 \cdot 10^{-2}$	$4.02 \cdot 10^{-2}$	0.98	0.98
0.02	8	1.6	$1.96 \cdot 10^{-2}$	$2.02 \cdot 10^{-2}$	0.98	0.99

Resolution			Relative error		Convergence rates	
Δx	λ	μ	l_2	l_∞	p_2	p_∞
0.04	16	1.62	0.11	0.11	-	-
0.04	8	0.82	$2.88 \cdot 10^{-2}$	$2.66 \cdot 10^{-2}$	1.93	2.05
0.02	16	3.2	$2.89 \cdot 10^{-2}$	$2.67 \cdot 10^{-2}$	1.93	2.04
0.02	8	1.6	$7.35 \cdot 10^{-3}$	$6.64 \cdot 10^{-3}$	1.95	2.03

Table 2: Errors for the solid body rotation test, methods SL1 (upper), SL2s (middle) and SL2 (lower) on a structured mesh.

While the behaviour of the SL2 scheme is entirely analogous to that of the structured mesh case, the SL2s method shows in this case little error reduction when the spatial resolution is kept fixed.

6.3 Reaction–diffusion equations

Following [15], we consider the Allen–Cahn equation

$$c_t = \nu \Delta c - c^3 + c$$

on the domain $\Omega = (0, 1) \times (0, 1)$, with periodic boundary conditions and for $t \in [0, 2]$. As in [15], we take the initial datum

$$c_0(x, y) = \sin(2\pi x) \sin(2\pi y)$$

and a reference solution is computed by a pseudo-spectral Fourier discretization in space, see e.g. [8], and a fourth order Runge–Kutta scheme in time with a very large number of time steps. The results

Resolution			Relative error		Convergence rates	
Δx	λ	μ	l_2	l_∞	p_2	p_∞
0.04	16	1.62	$2.39 \cdot 10^{-2}$	$2.25 \cdot 10^{-2}$	-	-
0.04	8	0.82	$2.72 \cdot 10^{-2}$	$2.84 \cdot 10^{-2}$	0.19	0.34
0.02	16	3.2	$7.20 \cdot 10^{-3}$	$6.32 \cdot 10^{-3}$	1.73	1.83
0.02	8	1.6	$2.48 \cdot 10^{-3}$	$2.59 \cdot 10^{-3}$	3.46	3.45

Resolution			Relative error		Convergence rates	
Δx	λ	μ	l_2	l_∞	p_2	p_∞
0.04	16	1.62	0.129	0.139	-	-
0.04	8	0.82	$4.02 \cdot 10^{-2}$	$4.42 \cdot 10^{-2}$	1.68	1.65
0.02	16	3.2	$2.88 \cdot 10^{-2}$	$2.56 \cdot 10^{-2}$	2.16	2.44
0.02	8	1.6	$7.70 \cdot 10^{-3}$	$8.08 \cdot 10^{-3}$	2.38	2.45

Table 3: Errors for the solid body rotation test, methods SL2s (upper) and SL2 (lower) on an unstructured mesh.

are reported in Table 4, for the values $\nu = 0.01$ and $\nu = 0.05$ of the diffusion parameter, respectively. In this case, only unstructured meshes were considered and the reference solution was interpolated onto the unstructured mesh nodes using a higher order interpolation procedure. Both tests show a quadratic order of convergence.

6.4   Advection–diffusion–reaction systems

We consider in this case a set of four coupled advection–diffusion–reaction equations of the form (2)

$$\frac{\partial c_k}{\partial t} + u \cdot \nabla c_k - \nu \Delta c_k = f_k(c_1, \ldots, c_4) \quad k = 1, \ldots, 4 \qquad (36)$$

on the square domain $\Omega = (-5, 5) \times (-5, 5)$ and on the time interval $t \in [0, 5]$. The advection field is given by coefficients $u = (-\omega y, \omega x)$, $\omega = 2\pi/10$, while the diffusion coefficient is set as $\nu = 0.01$. The reaction terms are given by

$$\begin{aligned}
f_1 &= (c_1 - c_1 c_2) - (c_1 - c_3)/5 \\
f_2 &= -2(c_2 - c_1 c_2) - (c_2 - c_4)/5 \\
f_3 &= 2(c_3 - c_3 c_4) \\
f_4 &= -4(c_4 - c_3 c_4),
\end{aligned}$$

Resolution			Relative error		Convergence rates	
Δx	Δt	μ	l_2	l_∞	p_2	p_∞
0.04	0.1	0.62	$1.10 \cdot 10^{-3}$	$1.31 \cdot 10^{-3}$	-	-
0.02	0.05	1.25	$2.72 \cdot 10^{-4}$	$2.98 \cdot 10^{-4}$	2.02	2.14
0.01	0.025	2.5	$6.53 \cdot 10^{-5}$	$7.06 \cdot 10^{-5}$	2.06	2.08

Resolution			Relative error		Convergence rates	
Δx	Δt	μ	l_2	l_∞	p_2	p_∞
0.04	0.1	0.62	$2.82 \cdot 10^{-2}$	$4.01 \cdot 10^{-2}$	-	-
0.02	0.05	1.25	$7.13 \cdot 10^{-3}$	$8.47 \cdot 10^{-3}$	1.98	2.24
0.01	0.025	2.5	$1.97 \cdot 10^{-3}$	$2.20 \cdot 10^{-3}$	1.86	1.94

Table 4: Error for the Allen–Cahn test with $\nu = 0.01$ (upper) and $\nu = 0.05$ (lower), second order method SL2 on an unstructured mesh.

which represent two coupled Lotka–Volterra prey-predator systems. As initial datum for c_1, c_3, the function

$$
c_0(x,y) = \begin{cases} \cos\left(2\pi[(x+2.5)^2 + y^2)]\right) & \text{for } (x+2.5)^2 + y^2 \leq \frac{1}{4} \\ \\ 0 & \text{for } (x+2.5)^2 + y^2 > \frac{1}{4} \end{cases}
$$

was considered, while the initial datum for c_2, c_4, was taken to be equal to $3c_0$. In this test, only a structured mesh was considered with constant steps $\Delta x = \Delta y = 1/20$. A reference solution is computed by a pseudo-spectral Fourier discretization in space and a fourth order Runge–Kutta scheme in time, using a very large number of time steps. The reference solution is reported for two sample components in Figure 2, while the absolute error distributions obtained for the same components with the second order method SL2 (14) using cubic interpolation, using a timestep corresponding to $\lambda \approx 7$ and $\mu \approx 1/2$, are shown in Figure 3. As a reference, the errors for a second order finite difference approximation of (36) using a second order Runge–Kutta scheme in time with a time step 20 times smaller are shown in Figure 4, while the errors obtained using a fourth order finite difference approximation for the advection term in (36) with a third order Runge–Kutta scheme in time are displayed in Figure 5, again computed with a time step 20 times smaller than that used for the SL2 method. It can be seen that the SL2 method allows to achieve errors of the same order of magnitude as those of the third order Runge–Kutta in time, while allowing for a much larger time step without solving large algebraic systems.
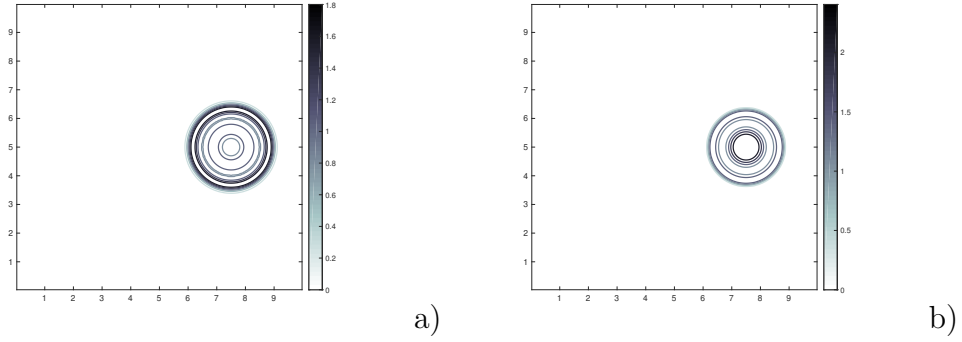
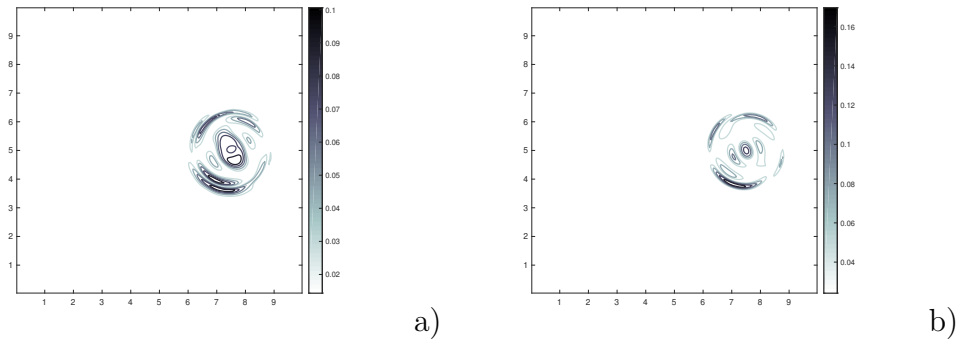Figure 2: Reference solutions for problem (36), a) component c_3, b) component c_4 at time $T = 5$.

Figure 3: Absolute errors of second order SL2 method for problem (36), a) component c_3, b) component c_4 at time $T = 5$.
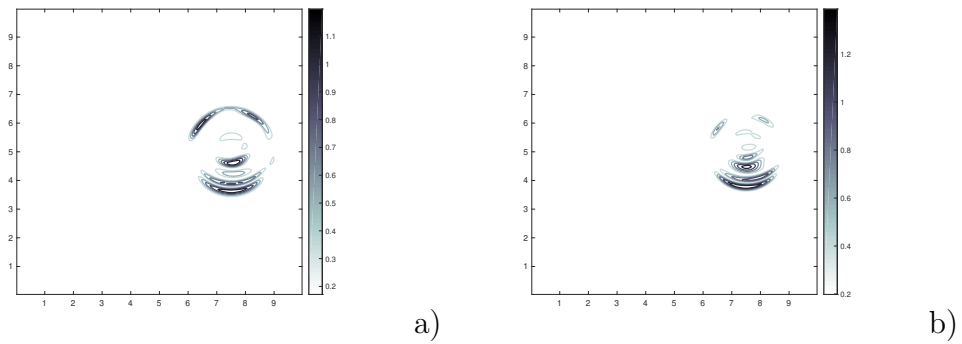

Figure 4: Absolute errors of second order finite difference method for problem (36), a) component c_3, b) component c_4 at time $T = 5$.
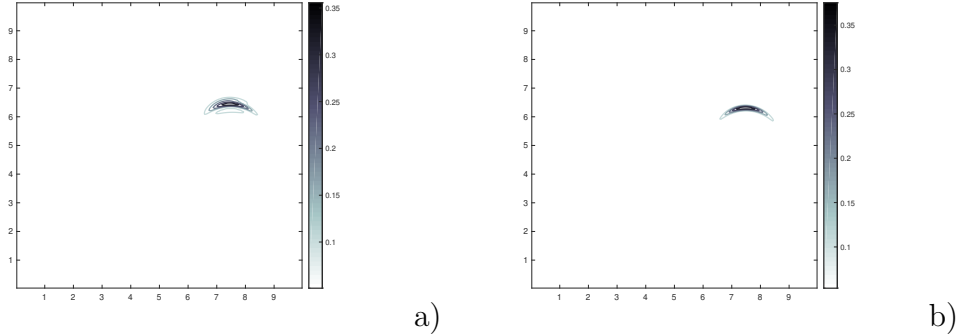
22

Figure 5: Absolute errors of fourth order finite difference method for problem (36), a) component c_3, b) component c_4 at time $T = 5$.

6.5 Advection–diffusion equation, nonhomogeneous boundary conditions

In this last set of numerical experiments, we consider nonhomogeneous, possibly time-dependent Dirichlet boundary conditions in four cases: pure diffusion, constant advection–diffusion, solid body rotation with diffusion and advection–diffusion on a nonconvex domain. In all these tests, we have used an unstructured mesh. In the first three cases, we consider $\Omega = (-1, 1) \times (-1, 1)$, final time $T = 1$ and an initial condition in the form of a Gaussian centered at $(x_0, y_0) = (0.5, 0)$, with $\sigma = 0.1$. In Fig.1, we show the space meshes $\mathcal{G}_{\Delta x}$ and $\mathcal{G}_h$ corresponding to the steps $\Delta x = 0.04$, $h = 0.5$, which were used to compute the results in the first two rows of Tables 5-7. In order to have a reference solution to compare with, we compute the exact solution on the whole of $\mathbb{R}^2$ and enforce its values at the boundary as boundary conditions, so that $b(x, y, t) = c(x, y, t)$ for $(x, y) \in \partial\Omega$, $t \in [0, T]$. For all the three cases, we have set $\nu = 0.05$ and $T = 1$. In the second and third test, the advection field has been chosen as $u = (1, 0)$, and $u = (-2\pi y, 2\pi x)$, respectively. Tables 5-7 report the numerical errors obtained by the SL2 scheme in these tests, showing in all cases at least a quadratic convergence.

We finally consider the advection–diffusion equation with $\nu = 0.001$, on the domain $\Omega = ([0, 1] \times [0, 0.4]) \backslash B_{r_0}(x_0, y_0)$, where $B_{r_0}(x_0, y_0)$ denotes a circle with radius $r_0 = 0.05$ centered in $(x_0, y_0) = (0.1, 0.2)$. The initial datum is $c_0(x, y) = 0$ and the boundary condition

$$b(x, y, t) = \begin{cases} y(0.4 - y)\frac{4}{0.4^2} & (x, y) \in \{0\} \times [0, 0.4], t \in [0, T] \\ 1 & (x, y) \in \partial B_r(x_0), t \in [0, T] \\ 0 & \text{otherwise.} \end{cases}$$

23

Resolution			Relative error		Convergence rates	
Δx	μ	h	l_2	l_∞	p_2	p_∞
0.04	1.56	0.5	$4.70 \cdot 10^{-3}$	$1.39 \cdot 10^{-2}$	-	-
0.04	0.78	0.5	$3.18 \cdot 10^{-3}$	$1.06 \cdot 10^{-2}$	-	-
0.02	3.12	0.33	$3.71 \cdot 10^{-4}$	$1.01 \cdot 10^{-3}$	3.66	3.78
0.02	1.56	0.33	$4.35 \cdot 10^{-4}$	$9.57 \cdot 10^{-4}$	2.87	3.47

Table 5: Errors and convergence rates for the pure diffusion problem with nonhomogeneous Dirichlet conditions, SL2 method, unstructured mesh

Resolution				Relative error		Convergence rates	
Δx	λ	μ	h	l_2	l_∞	p_2	p_∞
0.04	1.25	1.56	0.5	$7.35 \cdot 10^{-3}$	$1.18 \cdot 10^{-2}$	-	-
0.04	0.625	0.78	0.5	$8.35 \cdot 10^{-3}$	$1.32 \cdot 10^{-2}$	-	-
0.02	1.25	3.12	0.33	$3.76 \cdot 10^{-4}$	$7.59 \cdot 10^{-4}$	4.29	3.96
0.02	0.625	1.56	0.33	$2.64 \cdot 10^{-4}$	$5.58 \cdot 10^{-4}$	4.98	4.56

Table 6: Errors and convergence rates for the advection–diffusion problem with nonhomogeneous Dirichlet conditions, SL2 method, unstructured mesh.

Resolution				Relative error		Convergence rates	
Δx	λ	μ	h	l_2	l_∞	p_2	p_∞
0.04	7.85	1.56	0.5	$5.62 \cdot 10^{-2}$	$6.09 \cdot 10^{-2}$	-	-
0.04	3.92	0.78	0.5	$1.49 \cdot 10^{-2}$	$1.60 \cdot 10^{-2}$	-	-
0.02	7.85	3.12	0.33	$1.49 \cdot 10^{-2}$	$8.98 \cdot 10^{-2}$	1.91	-
0.02	3.92	1.56	0.33	$3.43 \cdot 10^{-3}$	$3.61 \cdot 10^{-3}$	2.12	2.15

Table 7: Errors and convergence rates for the solid body rotation problem with nonhomogeneous Dirichlet conditions, SL2 method, unstructured mesh.

The velocity field $u(x, y)$ is given by

$$u(x, y) = \left(u_0 + \frac{u_0 r_0^3}{2r^3} - \frac{3u_0 r_0^3 (x - x0)^2}{2r^5}, -\frac{3r_0^3 u_0 (x - x0)(y - y0)}{2r^5} \right),$$

where we set $u_0 = 0.2$ and $r^2 = (x - x_0)^2 + (y - y_0)^2$. In Fig. 6, we show the domain Ω, discretized using a Delaunay mesh $\mathcal{G}_{\Delta x}$ with $\Delta x = 0.1$, refined around the circular hole. In Fig. 7, we show the numerical solution computed with SL2 with time step $\Delta t = 0.005$ for time $t = 0.5, 1, 2, 3$. The nonhomogeneus boundary condition are computed by extrapolation with an extra grid $\mathcal{G}_h$ with $h = 1.5\sqrt{\Delta t}$. In this case, the additional mesh $\mathcal{G}_h$ has been built around the circular
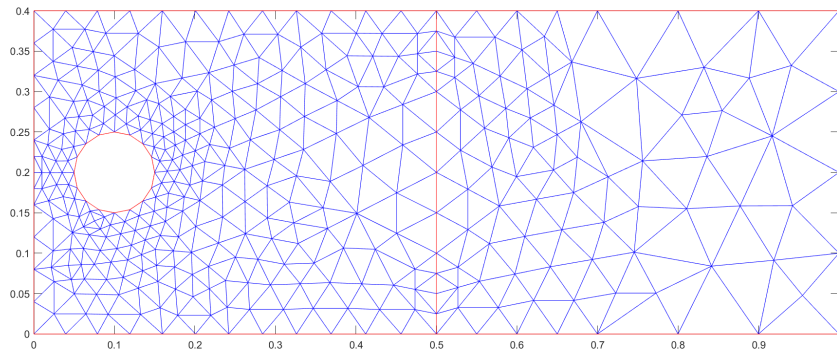
Figure 6: Unstructured mesh for the non-convex problem

hole, as well as along the external rectangular boundary. Note that, in spite of the discontinuity of the initial configuration and the sharp boundary layer around the hole, the boundary condition is smoothly propagated in the interior of the domain.

7   Conclusions

A family of fully semi-Lagrangian approaches for the discretization of advection–diffusion–reaction systems has been proposed, which extend the methods outlined in [3], [4] to full second order accuracy. The stability and convergence of the basic second order method has been analyzed. The proposed methods have been validated on a number of classical benchmarks, on both structured and unstructured meshes. Numerical results show that these methods yield good quantitative agreement with reference numerical solutions, while being superior in efficiency to standard implicit approaches and to approaches in which the SL method is only used for the advection term. In future developments, the proposed method will be extended to higher order discretizations along the lines of [33] and will be applied to the development of second order fully semi-Lagrangian methods for the Navier-Stokes equations along the lines of [2],[4].
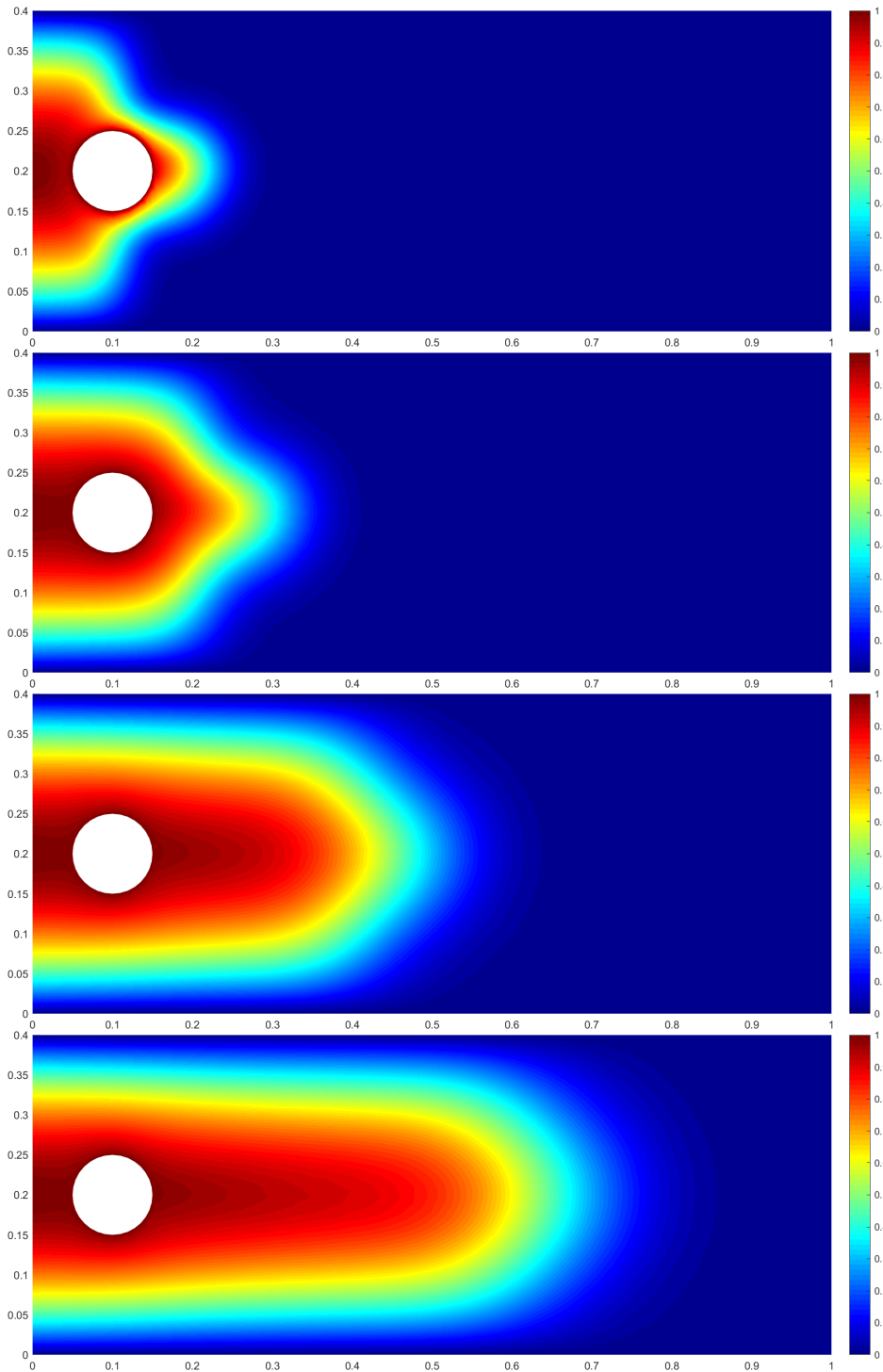
Acknowledgements

Figure 7: Numerical solution at time $t = 0.5, 1, 2, 3$

26

References

[1] L. Bonaventura. A semi-implicit, semi-Lagrangian scheme using the height coordinate for a nonhydrostatic and fully elastic model of atmospheric flows. *Journal of Computational Physics*, 158:186–213, 2000.

[2] L. Bonaventura, E. Calzola, E. Carlini, and R. Ferretti. A fully semi-Lagrangian method for the Navier-Stokes equations in primitive variables. In *Proceedings of the 2017 Finite Elements in Flows Conference, Rome*. Springer Verlag, 2020.

[3] L. Bonaventura and R. Ferretti. Semi-Lagrangian methods for parabolic problems in divergence form. *SIAM Journal of Scientific Computing*, 36:A2458 – A2477, 2014.

[4] L. Bonaventura, R. Ferretti, and L. Rocchi. A fully semi-Lagrangian discretization for the 2D Navier-Stokes equations in the vorticity–streamfunction formulation. *Applied Mathematics and Computation*, 323:132–144, 2018.

[5] L. Bonaventura, R. Redler, and R. Budich. *Earth System Modelling 2: Algorithms, Code Infrastructure and Optimisation.* Springer Verlag, New York, 2012.

[6] L. Bonaventura and A. Della Rocca. Unconditionally strong stability preserving extensions of the TR-BDF2 method. *Journal of Scientific Computing*, 70:859–895, 2017.

[7] M. Camilli and M. Falcone. An approximation scheme for the optimal control of diffusion processes. *Mathematical Modelling and Numerical Analysis*, 29:97–122, 1995.

[8] C. Canuto, M.Y. Hussaini, A. Quarteron, and T.A. Zang. *Spectral methods: Fundamentals in single domains.* Springer Science & Business Media, 2006.

[9] V. Casulli. Semi-implicit finite difference methods for the two dimensional shallow water equations. *Journal of Computational Physics*, 86:56–74, 1990.

[10] V. Casulli and E. Cattani. Stability, accuracy and efficiency of a semi-implicit method for three-dimensional shallow water flow. *Computers and Mathematics with Applications*, 27(4):99–112, 1994.

[11] J. Coté and A. Staniforth. A two time level semi-Lagrangian semi-implicit scheme for spectral models. *Monthly Weather Review*, 116:2003–2012, 1988.

[12] C. Erath, P.H. Lauritzen, J.H. Garcia, and H.M. Tufo. Integrating a scalable and efficient semi-Lagrangian multi-tracer transport scheme in HOMME. *Procedia Computer Science*, 9:994–1003, 2012.

[13] C. Erath, M.A. Taylor, and R.D. Nair. Two conservative multi-tracer efficient semi-Lagrangian schemes for multiple processor systems integrated in a spectral element (climate) dynamical core. *Communications in Applied and Industrial Mathematics*, 7:74–98, 2016.

[14] M. Falcone and R. Ferretti. *Semi-Lagrangian Approximation Schemes for Linear and Hamilton–Jacobi Equations.* SIAM, 2013.

[15] X. Feng, H. Song, T. Tang, and J. Yang. Nonlinear stability of the implicit-explicit methods for the Allen-Cahn equation. *Inverse Problems and Imaging*, 7:679–695, 2013.

[16] R. Ferretti. A technique for high-order treatment of diffusion terms in semi-Lagrangian schemes. *Communications in Computational Physics*, 8:445–470, 2010.

[17] R. Ferretti. On the relationship between semi-Lagrangian and Lagrange–Galerkin schemes. *Numerische Mathematik*, 124:31–56, 2013.

[18] R. Ferretti and M. Mehrenberger. Stability of semi-Lagrangian schemes of arbitrary odd degree under constant and variable advection speed. *Mathematics of Computation*, to appear.

[19] P.E. Kloeden and E. Platen. *Numerical solution of stochastic differential equations*, volume 23 of *Applications of Mathematics (New York)*. Springer-Verlag, Berlin, 1992.

[20] J.D. Lambert. *Numerical methods for ordinary differential systems.* Wiley, 1991.

[21] R. J. Leveque. *Finite Volume Methods for Hyperbolic Problems.* Cambridge University Press, Cambridge, UK, 2002.

[22] G.N. Milstein. The probability approach to numerical solution of nonlinear parabolic equations. *Numerical Methods for Partial Differential Equations*, 18:490–522, 2002.

[23] G.N. Milstein and M.V. Tretyakov. Numerical algorithms for semilinear parabolic equations with small parameter based on approximation of stochastic equations. *Mathematics of Computation*, 69:237–567, 2000.

[24] G.N. Milstein and M.V. Tretyakov. Numerical solution of the Dirichlet problem for nonlinear parabolic equations by a proba-

bilistic approach. *IMA Journal of Numerical Analysis*, 21:887–917, 2001.

[25] G.N. Milstein and M.V. Tretyakov. *Stochastic numerics for mathematical physics*. Springer Science & Business Media, 2013.

[26] J. Pudykiewicz and A. Staniforth. Some properties and comparative performance of the semi-Lagrangian method of Robert in the solution of the advection diffusion equation. *Atmosphere-Ocean*, 22:283–304, 1984.

[27] Alfio Quarteroni and Alberto Valli. *Numerical approximation of partial differential equations*. Springer Verlag, 1994.

[28] A. Robert. A semi-Lagrangian and semi-implicit numerical integration scheme for the primitive meteorological equations. *Journal of the Meteorological Society of Japan*, 60:319–325, 1982.

[29] G. Rosatti, D. Cesari, and L. Bonaventura. Semi-implicit, semi-Lagrangian environmental modelling on Cartesian grids with cut cells. *Journal of Computational Physics*, 204:353–377, 2005.

[30] A. Staniforth and J. Coté. Semi-Lagrangian integration schemes for atmospheric models-a review. *Monthly Weather Review*, 119:2206–2223, 1991.

[31] C. Temperton, M. Hortal, and A. Simmons. A two-time-level semi-Lagrangian global spectral model. *Quarterly Journal of the Royal Meteorological Society*, 127:111–127, 2001.

[32] C. Temperton and A. Staniforth. An efficient two-time-level semi-Lagrangian semi-implicit integration scheme. *Quarterly Journal of the Royal Meteorological Society*, 113:1025–1039, 1987.

[33] G. Tumolo and L. Bonaventura. A semi-implicit, semi-Lagrangian, DG framework for adaptive numerical weather prediction. *Quarterly Journal of the Royal Meteorological Society*, 141:2582–2601, 2015.

[34] G. Tumolo, L. Bonaventura, and M. Restelli. A semi-implicit, semi-Lagrangian, $p-$adaptive discontinuous Galerkin method for the shallow water equations. *Journal of Computational Physics*, 232:46–67, 2013.

[35] N.P. Wedi, P. Bauer, M. Diamantakis, M. Hamrud, S. Malardel, K. Mogensen, G. Mozdzynski, and P.K. Smolarkiewicz. The modelling infrastructure of the Integrated Forecasting System: Recent advances and future challenges. Technical Report 760, ECMWF, 2015.

MOX Technical Reports, last issues

Dipartimento di Matematica
Politecnico di Milano, Via Bonardi 9 - 20133 Milano (Italy)

09/2020   Rea, F.; Ieva, F.,; Pastorino, U.; Apolone, G.; Barni, S.; Merlino, L.; Franchi, M.; Corrao, G.
*Number of lung resections performed and long-term mortality rates of
patients after lung cancer surgery: evidence from an Italian investigation*

08/2020   Antonietti, P. F.; Facciolà, C.; Verani, M.
*Polytopic Discontinuous Galerkin methods for the numerical modelling of
flow in porous media with networks of intersecting fractures*

05/2020   Artioli, E.; Beiraoda Veiga, L.; Verani, M.
*An adaptive curved virtual element method for the statistical homogenization
of random fibre-reinforced composites*

06/2020   Domanin, M.; Piazzoli, G.; Trimarchi, S.; Vergara, C.
*Image-based displacements analysis and computational blood dynamics after
endovascular aneurysm repair*

07/2020   Fumagalli, A.; Scotti, A.
Reactive flow in fractured porous media

04/2020   Didkovskyi, O.; Azzone, G.; Menafoglio A.; Secchi P.
*Social and material vulnerability in the face of seismic hazard: an analysis of
the Italian case*

03/2020   Ferro, N.; Micheletti, S.; Perotto, S.
*Compliance-stress constrained mass minimization for topology optimization
on anisotropic meshes*

02/2020   Fresca, S.; Dede', L.; Manzoni, A.
*A comprehensive deep learning-based approach to reduced order modeling of
nonlinear time-dependent parametrized PDEs*

01/2020   Pozzi, S.; Vergara, C.
*Mathematical and numerical models of atherosclerotic plaque progression in
carotid arteries*

56/2019   Antonietti, P.F.; Berrone, S.; Borio A.; D'Auria A.; Verani, M.; Weisser, S.
Anisotropic a posteriori error estimate for the Virtual Element Method